

## Incorporation of Landmark Error Ellipsoids for Image Registration Based on Approximating Thin-Plate Splines\*

K. Rohr, R. Sprenkel, H.S. Stiehl

Universität Hamburg, Fachbereich Informatik, Arbeitsbereich Kognitive Systeme  
Vogt-Kölln-Str. 30, D-22527 Hamburg, Germany

We present an approach for elastic registration of 3D tomographic images which is based on a set of corresponding anatomical point landmarks and takes into account anisotropic landmark localization errors in form of 3D error ellipsoids. The 3D error ellipsoids are directly estimated from the image data. The performance of our approach is demonstrated for 2D and 3D MR images of the human brain.

### 1. INTRODUCTION

Nonrigid registration of 3D tomographic images of different modalities (e.g., CT and MR images) is a key issue for neurosurgery and radiotherapy planning. Here, we consider image registration based on a set of corresponding anatomical point landmarks and approximating thin-plate splines. With this approach it is possible to take into account landmark localization errors and thus to control the influence of the landmarks on the registration result. This is important for practical applications since landmark extraction is always prone to error, either in the case of interactive or automatic landmark localization. Our approximating thin-plate spline approach is an extension of the original interpolating thin-plate spline approach [1],[3] and has been introduced in [5],[6] for images of arbitrary dimension. The approach is based on functional analysis (regularization theory) and uses scalar weights to represent landmark localization errors. For a different approach to relax the interpolation condition see [2]. However, this approach has been not been related to a minimizing functional. Also, this approach has only been described for the 2D case and has only been applied to synthetic data.

One problem with our approach in [5],[6] is that scalar weights for the landmarks are only a coarse characterization of the localization errors. Generally, the errors are different in different directions and thus are anisotropic. Another problem is how to acquire the additional information about the landmark errors. Here, one approach is the utilization of prior knowledge about the localization errors of anatomical landmarks. Another possibility is to infer such information by analyzing the local intensity variations of the image.

In this contribution, we further extend our approach by incorporating covariance matrices of landmark position errors. For 3D images we have  $3 \times 3$  covariance matrices and

---

\*This work has been supported by Philips Research Hamburg, project IMAGINE (IMage- and Atlas-Guided Interventions in NEurosurgery).

we can represent the errors by 3D error ellipsoids. We show that the 3D error ellipsoids can directly be estimated from the image data. These ellipsoids characterize the local intensity variations at a landmark point and represent the minimal localization uncertainty of a landmark (Cramér-Rao bound). The estimated error ellipsoids are used as additional input to our extended approximating thin-plate spline approach. With this new approach it is possible to include different types of 3D point landmarks, e.g., ‘normal’ landmarks as well as ‘quasi-landmarks’. An example for quasi-landmarks are edge points. Such points are not uniquely definable in all directions, and they are used, for example, in the reference system of Talairach [7] to define the 3D bounding box of the brain. The incorporation of such landmarks is important since ‘normal’ point landmarks are hard to define, for example, at the outer parts of the brain.

In the following, we first present an extension of the approximating thin-plate spline approach to incorporate landmark error ellipsoids. Then, we describe an approach for estimating the error ellipsoids directly from image data. The performance of the whole scheme is demonstrated for 2D as well as 3D MR images.

## 2. APPROXIMATING THIN-PLATE SPLINES INCORPORATING LANDMARK ERROR ELLIPSOIDS

In [5],[6] we have introduced a point-based approach for nonrigid matching of medical images using approximating thin-plate splines which is based on the mathematical work in [8]. To find the transformation  $\mathbf{u}$  between two images of dimension  $d$  we assume to have two sets of  $n$  landmarks  $\mathbf{p}_i$  and  $\mathbf{q}_i$ ,  $i = 1 \dots n$  in the first and second image, respectively, as well as information about the landmark localization error in terms of scalar weights  $\sigma_i^2$ . Then,  $\mathbf{u}$  results as the solution of a minimizing functional which measures the distance between the two landmark sets and the smoothness of the transformation:

$$J_\lambda(\mathbf{u}) = \frac{1}{n} \sum_{i=1}^n \frac{|\mathbf{q}_i - \mathbf{u}(\mathbf{p}_i)|^2}{\sigma_i^2} + \lambda J_m^d(\mathbf{u}). \quad (1)$$

This functional can be separated into a sum of functionals which only depend on one component of  $\mathbf{u}$ . The smoothness term for one component can generally be written as

$$J_m^d(u) = \sum_{\alpha_1 + \dots + \alpha_d = m} \frac{m!}{\alpha_1! \dots \alpha_d!} \int_{\mathbb{R}^d} \left( \frac{\partial^m u}{\partial x_1^{\alpha_1} \dots \partial x_d^{\alpha_d}} \right)^2 d\mathbf{x}, \quad (2)$$

where  $m$  is the order of the involved derivatives of  $\mathbf{u}$ . The relative weight between the two terms in (1) is determined by the regularization parameter  $\lambda > 0$ . The solution to minimizing this functional can be stated analytically as

$$u(\mathbf{x}) = \sum_{i=1}^M a_i \phi_i(\mathbf{x}) + \sum_{i=1}^n w_i U_i(\mathbf{x}), \quad (3)$$

with polynomials  $\phi_i$  up to order  $m - 1$  and suitable radial basis functions  $U_i = U(\cdot, \mathbf{p}_i)$  as defined in [8].

The coefficient vectors  $\mathbf{a} = (a_1, \dots, a_M)^T$  and  $\mathbf{w} = (w_1, \dots, w_n)^T$  of the transformation can be computed through the following system of linear equations:

$$\begin{aligned} (\mathbf{K} + n\lambda\mathbf{W}^{-1})\mathbf{w} + \mathbf{P}\mathbf{a} &= \mathbf{v} \\ \mathbf{P}^T\mathbf{w} &= 0, \end{aligned} \quad (4)$$

where  $\mathbf{v}$  is the column vector of one component of the coordinates of the target points  $\mathbf{q}_i$ ,  $K_{ij} = U_i(\mathbf{p}_j)$ , and  $P_{ij} = \phi_j(\mathbf{p}_i)$ . The matrix

$$\mathbf{W}^{-1} = \text{diag}\{\sigma_1^2, \dots, \sigma_n^2\} \quad (5)$$

contains the scalar weights representing isotropic landmark localization errors.

This approach can further be extended when replacing the scalar weights  $\sigma_i^2$  by covariance matrices  $\Sigma_i$  representing anisotropic landmark localization errors. Now our functional reads as

$$J_\lambda(\mathbf{u}) = \frac{1}{n} \sum_{i=1}^n (\mathbf{q}_i - \mathbf{u}(\mathbf{p}_i))^T \Sigma_i^{-1} (\mathbf{q}_i - \mathbf{u}(\mathbf{p}_i)) + \lambda J_m^d(\mathbf{u}). \quad (6)$$

The solution to minimizing this functional is obtained by reducing it to the known thin-plate spline approximation theory in [8] and thus can also be stated in analytic form. The computational scheme to compute the coefficient vectors of the transformation  $\mathbf{u}$  is analogous to (4), while a separation is no longer possible. The weighting matrix now represents the covariance matrices  $\Sigma_i, i = 1 \dots n$  of the landmarks through

$$\mathbf{W}^{-1} = \text{diag}\{\Sigma_1, \dots, \Sigma_n\}, \quad (7)$$

which is a block-diagonal matrix. Note, that the  $\Sigma_i$  represent the localization errors of corresponding landmark pairs. Thus, we have to combine the covariance matrices of corresponding landmarks. If we assume that the corresponding two covariance matrices only slightly depend on the nonlinear part of the transformation, then we can combine these matrices by applying a linear transformation which allows for rotation, scale, and shear. If we can further assume that the images have approximately the same orientation, scale, and shear then we can simply add the two covariance matrices.

### 3. ESTIMATION OF LANDMARK ERROR ELLIPSOIDS

Having extended our approximating thin-plate spline approach from scalar weights to full covariance matrices, we now have the problem of providing our algorithm with the necessary information. One possibility is to use prior knowledge about the localization errors of anatomical landmarks. In this contribution, however, we suggest a different approach which allows to estimate the 3D covariance matrices at landmarks directly from the image data. In this case, the covariance matrices represent the minimal stochastic localization error (Cramér-Rao bound). The corresponding error ellipsoids characterize the local intensity variations at a considered landmark point. Let  $\sigma_n^2$  denote the variance of the image noise,  $m$  the number of voxels involved in a local 3D window, and  $\nabla g$  the 3D image gradient. Then, we can relate the matrix  $\underline{C}_g = \overline{\nabla g (\nabla g)^T}$ , which captures the local intensity variations of the 3D window, to the minimal localization uncertainty of the center of the window  $\mathbf{x}$  characterized by the covariance matrix  $\underline{\Sigma}$ :

$$\underline{\Sigma} = \frac{\sigma_n^2}{m} \underline{C}_g^{-1}. \quad (8)$$

From (8) we can derive the 3D error ellipsoid of the position estimate with main axes  $\sigma_x, \sigma_y$ , and  $\sigma_z$ . Based on the above relation we can distinguish different types of landmark points in 3D tomographic images. This approach is a 3D extension of the 2D

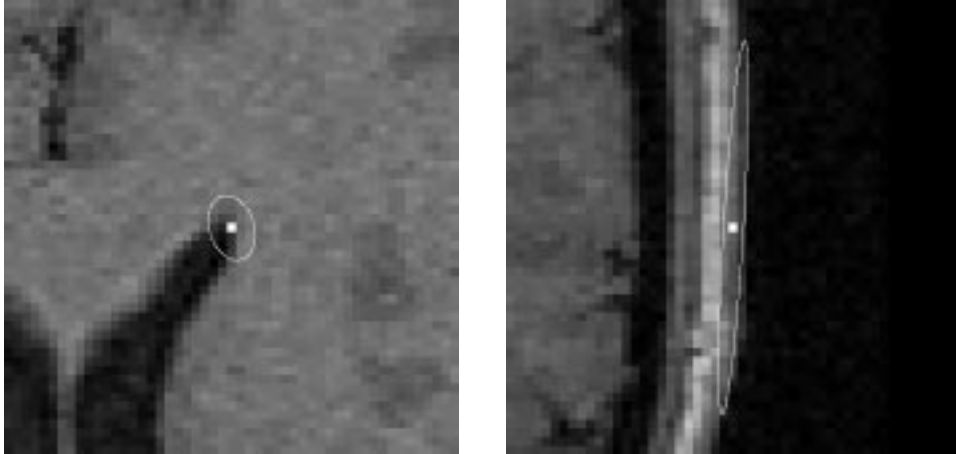


Figure 1. Estimated 2D error ellipses (enlarged by a factor of 30) for a 2D MR dataset: frontal tip of ventricle system (left) and edge point at the outer contour of the head (right)

approach in [4] which has been applied within the field of photogrammetry. In our case, 3D landmarks with locally high intensity variations in all directions, i.e. strongly curved intensity surfaces, have low localization uncertainties in all directions and we will refer to them as ‘normal’ point landmarks. Landmarks at edges have high localization uncertainties along the edge but low localization uncertainties perpendicular to the edge. Such landmarks will be denoted as ‘quasi-landmarks’ since they are not uniquely definable in all directions. They are used, for example, in the reference system of Talairach [7] to define the 3D bounding box of the brain. Note, that edges in 3D images are generally surfaces whereas in 2D they are lines. Finally, ‘normal’ landmarks and ‘quasi-landmarks’ can be distinguished from points in homogeneous regions where we have high localization uncertainties in all directions.

As an example, we show in Fig. 1 the estimated error ellipses of the frontal tip of the ventricle system as well as for an edge point at the outer contour of the head within a 2D MR dataset. The selected points are examples for ‘normal’ landmarks and ‘quasi-landmarks’. Note, that the error ellipses have been enlarged by a factor of 30 for visualization purposes. It can be seen that the error ellipse of the tip is small and close to a circle which means that the localization uncertainty for this point is low in arbitrary directions. For the edge point, however, the error ellipse is largely elongated and indicates a large localization uncertainty along the contour and a low localization uncertainty perpendicular to the contour. This is what we expect from the local intensity structure at the considered points. In Fig. 2 the 3D error ellipsoid for the genu of corpus callosum within a 3D MR dataset has been represented by three orthogonal views (sagittal, axial, coronal). Whereas the sagittal view exhibits anisotropic localization uncertainties, in the axial and coronal view the localization uncertainties in different directions are more similar.

#### 4. EXPERIMENTAL RESULTS

Our extended approximating thin-plate spline approach has been applied to elastic registration of tomographic images of the human brain. Fig. 3 shows the registration

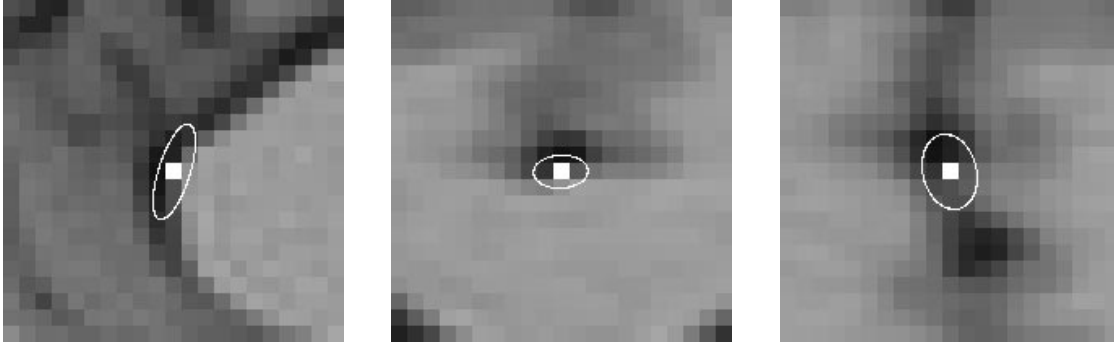


Figure 2. Estimated 3D error ellipsoid (enlarged by a factor of 30) for landmark point at genu of corpus callosum within a 3D MR dataset (orthogonal views: sagittal (left), axial (middle), coronal (right))

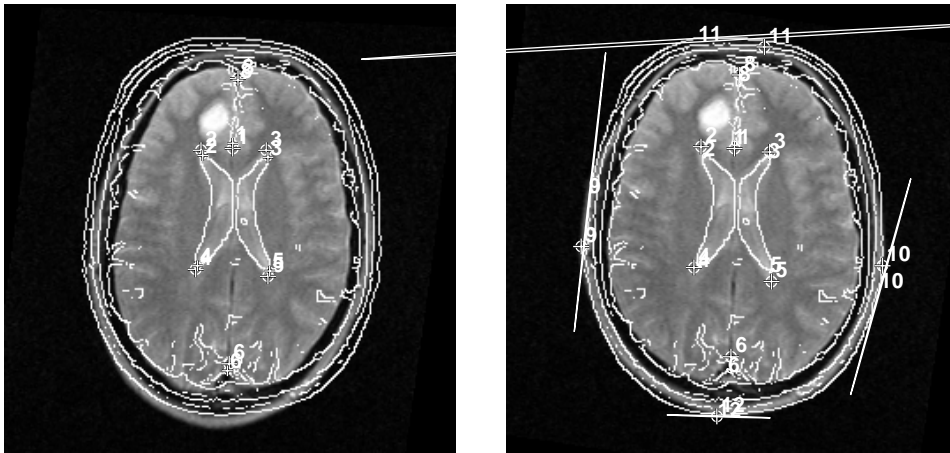


Figure 3. Registration result of two 2D MR datasets: ‘normal’ landmarks and equal scalar weights (left), ‘normal’ landmarks, ‘quasi-landmarks’ and estimated 2D error ellipses (right)

result of two 2D MR datasets of different human brains. The edges of the second image have been overlaid onto the transformed first image. On the left side of Fig. 3 is given the result of our previous approach with  $m = d = 2$  using ‘normal’ landmarks and equal scalar weights to characterize the landmark localization errors. Using instead our new approach with additional ‘quasi-landmarks’ at the outer contour of the head while automatically estimating the error ellipses of all landmarks, then we obtain the result on the right side of Fig. 3. It can be seen that the combination of both types of landmarks significantly improves the registration accuracy, particularly at the outer contour of the brain.

In Fig. 4 we show an application of our new approach to 3D MR datasets (see slices 29 and 67 on the left and right side, respectively). We have used ‘normal’ landmarks as well as ‘quasi-landmarks’ as input to our elastic registration scheme and have estimated the corresponding 3D error ellipsoids directly from the image data. Also for these datasets we obtain a good registration result.

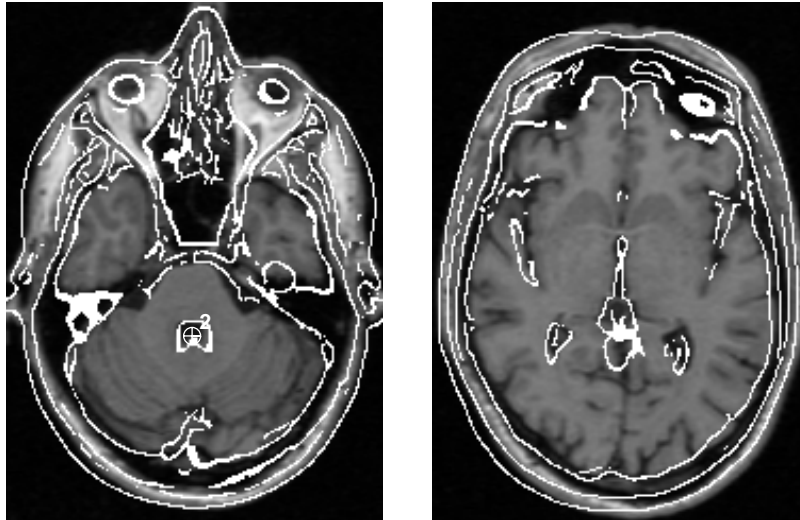


Figure 4. Registration result of two 3D MR datasets using ‘normal’ landmarks, ‘quasi-landmarks’ and estimated 3D error ellipsoids: slice 29 (left) and slice 67 (right)

## REFERENCES

1. F.L. Bookstein, “Principal Warps: Thin-Plate Splines and the Decomposition of Deformations”, *IEEE Trans. on Pattern Anal. and Machine Intell.* 11:6 (1989) 567-585
2. F.L. Bookstein, “Four metrics for image variation”, *Proc. 11th Internat. Conf. Information Processing in Medical Imaging (IPMI’89)*, In *Progress in Clinical and Biological Research*, Vol. 363, D. Ortendahl and J. Llacer (Eds.), Wiley-Liss New York, 1991, 227-240
3. A.C. Evans, W. Dai, L. Collins, P. Neelin, and S. Marrett, “Warping of a computerized 3-D atlas to match brain image volumes for quantitative neuroanatomical and functional analysis”, *Medical Imaging V: Image Processing*, 1991, San Jose, CA, Proc. SPIE 1445, M.H. Loew (Ed.), 236-246
4. W. Förstner, “A Feature Based Correspondence Algorithm for Image Matching”, *Intern. Arch. of Photogrammetry and Remote Sensing* 26-3/3 (1986) 150-166
5. K. Rohr, H.S. Stiehl, R. Sprengel, W. Beil, T.M. Buzug, J. Weese, and M.H. Kuhn, “Point-Based Elastic Registration of Medical Image Data Using Approximating Thin-Plate Splines”, *Proc. 4th Internat. Conf. Visualization in Biomedical Computing (VBC’96)*, Hamburg, Germany, Sept. 22-25, 1996, *Lecture Notes in Computer Science* 1131, K.H. Höhne and R. Kikinis (Eds.), Springer Berlin Heidelberg 1996, 297-306
6. R. Sprengel, K. Rohr, H.S. Stiehl, “Thin-Plate Spline Approximation for Image Registration” *18th Internat. Conf. IEEE Engineering in Medicine and Biology Society (EMBS’96)*, Oct. 31 - Nov. 3, 1996, Amsterdam, The Netherlands, CD-ROM Proceedings, Track Index 4.7.1 Image Registration
7. J. Talairach and P. Tournoux, *Co-planar Stereotactic Atlas of the Human Brain*, Georg Thieme Verlag Stuttgart New York 1988
8. G. Wahba, *Spline Models for Observational Data*, Society for Industrial and Applied Mathematics, Philadelphia, Pennsylvania, 1990